Article

Chinese Science Bulletin

SPECIAL TOPIC
Coseismic Deformation and Rupture Processes of the 2013 Lushan Earthquake

October 2013 Vol.58 No.28-29: 3444–3450
doi: 10.1007/s11434-013-6017-6

Source rupture process of Lushan M_S7.0 earthquake, Sichuan, China and its tectonic implications

ZHAO CuiPing[1*], ZHOU LianQing[1] & CHEN ZhangLi[2]

[1] *Institute of Earthquake Science, China Earthquake Administration, Beijing 100036, China;*
[2] *China Earthquake Administration, Beijing 100036, China*

Received June 9, 2013; accepted July 8, 2013; published online August 22, 2013

The source rupture process of the M_S7.0 Lushan earthquake was here evaluated using 40 long-period P waveforms with even azimuth coverage of stations. Results reveal that the rupture process of the Lushan M_S7.0 event to be simpler than that of the Wenchuan earthquake and also showed significant differences between the two rupture processes. The whole rupture process lasted 36 s and most of the moment was released within the first 13 s. The total released moment is 1.9×10^{19}N m with M_W=6.8. Rupture propagated upwards and bilaterally to both sides from the initial point, resulting in a large slip region of 40 km×30 km, with the maximum slip of 1.8 m, located above the initial point. No surface displacement was estimated around the epicenter, but displacement was observed about 20 km NE and SW directions of the epicenter. Both showed slips of less than 40 cm. The rupture suddenly stopped at 20 km NE of the initial point. This was consistent with the aftershock activity. This phenomenon indicates the existence of significant variation of the medium or tectonic structure, which may prevent the propagation of the rupture and aftershock activity. The earthquake risk of the left segment of Qianshan fault is worthy of attention.

Lushan earthquake, Wenchuan great earthquake, source rupture process, aftershock activity

Citation: Zhao C P, Zhou L Q, Chen Z L. Source rupture process of Lushan M_S7.0 earthquake, Sichuan, China and its tectonic implications. Chin Sci Bull, 2013, 58: 3444–3450, doi: 10.1007/s11434-013-6017-6

At 8:02 a.m. on April 20, 2013 (Beijing time), an earthquake of M_S7.0 struck Lushan County, Ya'an City, Sichuan Province, China. According to quick report from the CENC, it took place at 30.3°N 103°E at a depth of 13 km. The Lushan earthquake took place on the southwestern part of Longmenshan fault zone (LFZ), and it is the second devastating event occurred on the LFZ after the M_S8.0 Wenchuan earthquake in 2008. The distance between the two epicenters is about 100 km. By April 24, 2013, 196 people had been killed. The Lushan earthquake caused severe damage, as did the 2008 "5.12" Wenchuan earthquake and the M_S7.1 Yushu earthquake in 2010, which both took place in mainland China.

The source rupture process study of the 2008 Wenchuan earthquake reveals that the rupture propagated from the initial point (Yinxiu Town) towards the northeastern direction along the LFZ and caused a rupture about 330 km long within 120 s [1]. The early rupturing stage showed reverse faulting and later changed to right-lateral strike slip faulting, leaving 2 large slip areas along the LFZ on the surface. Aftershock activity also showed a unilateral pattern along the northeastern direction, consistent with the direction of rupture propagation. These seismological results were in accordance with the results of the post-earthquake investigation and of observations made during the disaster [2,3]. Evaluation of the source-rupture process using the digital seismic waveform data can provide information about the rupture scale, the way the fault moves, and the slip distribution on the fault within several hours of a strong earthquake. These estimations not only provide information regarding the seriously damaged areas and the way of dislocation but also information suitable for estimation of the scale of destruction and planning of rescue work. It can also provide information regarding the activity of the causative fault, the

*Corresponding author (email: zhaocp@seis.ac.cn)

tendency of future strong aftershocks. Key issues including the rupture pattern of the Lushan earthquake, its similarities and differences from the "5.12" Wenchuan earthquake which occurred on the same LFZ, as well as the tendency of risk of strong earthquakes along the LFZ, are main concerns after the occurrence of Lushan earthquake. Immediately after the Lushan earthquake, we estimated the preliminary rupture process pattern using a plane fault model, and the results were published on the webpage. In this paper, more data were used to improve the inversion result. The rupture features are further analyzed, differences from the Wenchuan earthquake and the tectonic meaning of the seismogenic fault reflected in the rupture process are discussed.

1 Tectonic background

The Longmenshan thrusting nappe structure zone is the boundary between the Bayan Har block in the Tibetan Plateau and the South China block to the east. It is also a tectonic boundary belt of two different crustal and lithosphere structures (Figure 1). This huge thrust tectonic belt was formed by the intense collision between the Bayan Har block and the South China block. On both sides of the Longmenshan fault zone, the crustal thickness varies from 35 km in the east Sichuan Basin to 70 km in the west. A variety of geophysical factors demonstrated strong gradient changes on LFZ sides, such as electrical structure [4], gravity field [5], seismic wave attenuation [6], and P-wave velocity structure [7].

The general strike of the LFZ is N45°E and NW-trending. From northwest to southeast, LFZ is composed of three main plow-like west-dipping faults zones, the Longmenshan-Houshan fault zone, the Longmenshan central fault zone, and the Longmenshan-Qianshan fault zone. Each zone is composed by several different sections [8]. Geological survey revealed that these three main faults zones have undergone a NW to SE thrusting movement accompanied by significant dextral strike-slip component since the late Quaternary.

The Lushan earthquake occurred in the southern section of the LFZ, where it developed many secondary thrust faults. Several NE-trending faults, Yanjing-Wulong, Shuangshi-Dachuan, Dayi, Pujiang-Xinjin, parallel from west to east (Figure 1). The Yanjin-Wulong fault is in the southern section of the Longmenshan central fault zone. The Shuangshi-Dachuan fault is in the southern part of the Longmenshan-Qianshan fault zone, and it is the southeastern boundary fault of the Longmenshan fault zone. The Dayi fault is a steeper buried fault in Sichuan Basin. One study revealed that, from west to east, the intensity of tectonic deformation decreases in the southern section of the Longmenshan fault zone [9]. The region between Yanjin-Wulong fault and Shuangshi-Dachuan fault experienced strong tectonic deformation. The area developed numerous thrust belts and

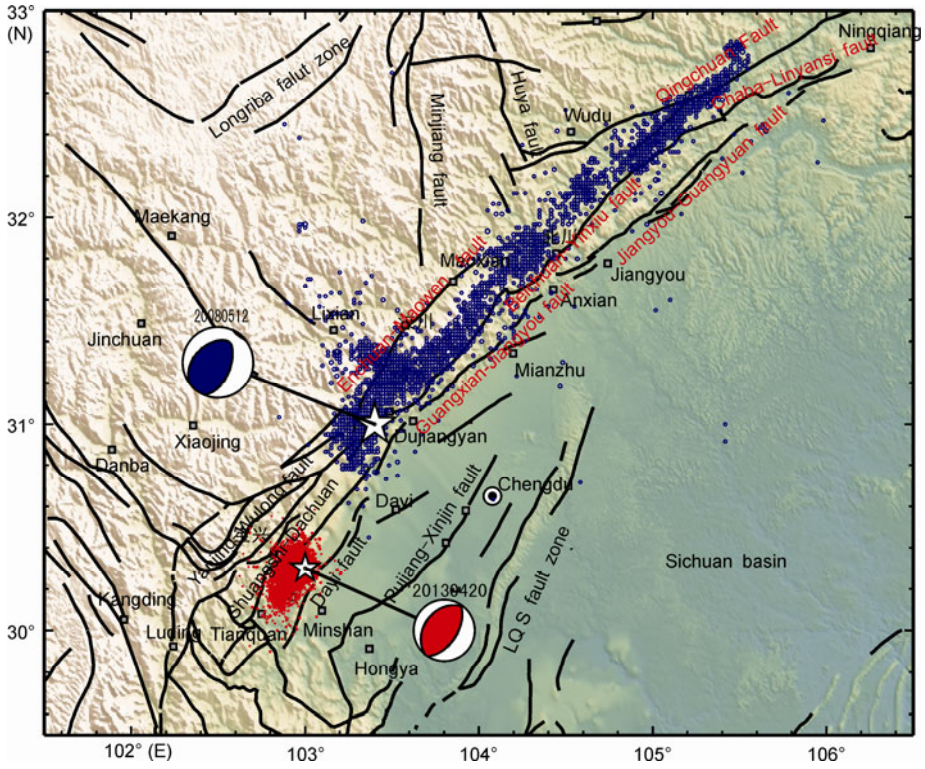

Figure 1 Focal mechanism and aftershock distribution of Lushan M_S7.0 earthquake on April 20, 2013 and the Wenchuan M_S8.0 earthquake on May 12, 2008. Large and small stars represent the epicenters of the Wenchuan and Lushan earthquakes, respectively. Blue circles are aftershocks of the Wenchuan earthquake, and red dots are aftershocks of the Lushan earthquake.

demonstrated a transition from ductile deformation to brittle deformation. Back-thrusting fault-block structures and fault-related folds developed between the Shuangshi-Dachuan and Dayi faults. The eastern region of the Dayi fault showed little intense deformation.

Lushan earthquake and its aftershocks took place between the Dayi fault (the buried fault) and the Shuangshi-Dachuan fault (Figure 1). Up until May 4, 2013, the relocation of Lushan earthquake sequence showed that aftershocks mainly occurred in a smaller range of 40 km in the northeast direction. There was an evident seismicity-empty segment between the Lushan and Wenchuan earthquake sequences.

2 Methods

In order to conduct rupture process inversion supposing a finite plane fault, the seismic fault is generally divided into many sub-faults. The whole source rupture process is then considered to be the summation of all these sub-events that can be regarded as point sources. The synthetic seismogram of an individual station is the summation of displacement excited by each sub-fault, and the displacement $D^i(t)$ at station i can be written as

$$D^i(t) = \sum_{j=1}^{N} M_j s_j(t) * g_j^i(t-\tau_{ij}), \quad (1)$$

where $D^i(t)$ is the displacement concluding the instrument response, M_j is the scalar seismic moment of the sub-fault j, N is the number of M_j, $S_j(t)$ is the source time function of sub-fault j, $g_j^i(t)$ is the green function of station i excited by the sub-fault j, τ_{ij} is the time delay of sub-fault j respect to the reference point (usually the starting point) and recorded by station i. τ_{ij} is estimated by eq. (2):

$$\tau_{ij} = \sqrt{x_j^2 + y_j^2}/V_r + (-x_j \cdot p_{ij} \cdot \cos\varphi_{ij}) + [-y_j \cdot [(1/v^2 - p_{ij}^2)^{1/2} \cdot \sin\delta] + p_{ij}\cos\delta \cdot \sin\varphi_{ij}, \quad (2)$$

where x_j and y_j are the distances between sub-fault j and the initial point along the strike and down the dip respectively. p_{ij} is the ray parameter from sub-fault j to the station i, and φ_{ij} is the value of azimuth of station i minus the strike of the fault. δ is the dip angle, Vr is the rupture velocity, v is Vp or Vs. Then the source-rupture process inversion is conducted by solving the over-determined equation (3):

$$\boldsymbol{GM} = \boldsymbol{D}, \quad (3)$$

where $\boldsymbol{D}$ represents the data vector consisting of observational data, $\boldsymbol{G}$ represents the coefficient vector considering the time delay. $\boldsymbol{M}$ is the solution vector composed of the N sub-faults. The Kikuchi and Kanamori method, which is based on a finite fault and the non-negative least square method, was used to restore the rupture scenario by fitting the observed waveform to the synthetic one in a time domain [10–13]. In order to obtain a stable solution, a smooth constraint was added alongside the non-negative prerequisite to keep the slip ratio of the neighbored sub-fault below a preset constant. The covariance of synthetic data with the observed data Var was defined as eq. (4):

$$Var = \sum_{j=1}^{N} \int \left[(d_j(t) - w_j(t))^2 \right] \mathrm{d}t \Big/ \sum_{j=1}^{N} \int [d_j(t)]^2 \mathrm{d}t, \quad (4)$$

where $d_j(t)$ and $w_j(t)$ represent the recorded data and synthetic data respectively.

3 Data and processing

Waveform data were downloaded from IRIS data center with an epicenter distance between 30°–90°. The data were subjected to further selection in terms of data quality and azimuth coverage. Forty far-field P waveforms were selected. As shown in Figure 2, the 40 stations evenly surrounded the Lushan epicenter. During inversion, the observed and synthetic data were both band-path filtered to 0.005–1.0 Hz. The duration of the P waveform data used was 50 s.

A plane fault model with strike= 231°, dip=42°, and slip =131° was used as the seismogenic fault, according to the moment inversion published by of Liu et al. (http://www.cea-igp.ac.cn/tpxw/266824.shtml). A rectangular section 100 km in length along the strike and 45 km in width down the dip with the initial point at the center, was chosen as the fault plane. It was divided into a series of sub-faults, each with a size of 10 km×5 km. The time window for each sub-fault was set into a series of triangle functions with a rise time and delay time of 4 seconds each. The rupture velocity was set to a value within the range of 2.5–3.0 km/s

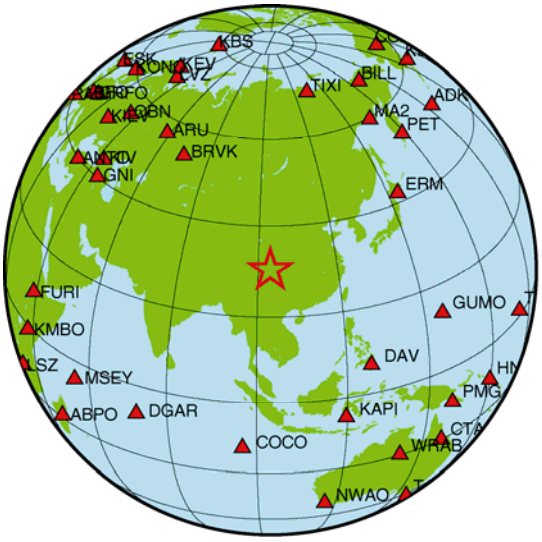

Figure 2 Epicenter of Lushan M_S7.0 earthquake (star) and stations used (triangle).

individually, and the proper rupture velocity was determined by the fitting variance of the observed data with synthetic data.

4 Results

The best fitted synthetic and observed waveform data are shown in Figure 3, with the fitting covariance *Var*= 0.25 and rupture velocity *V*r=3.0 km/s. According to the source time function (Figure 4), the rupture process lasted 30 s and consisted of 3 stages of moment scalar release, but most of the scalar moment was released within the first 13 s. The total released scalar seismic moment was 1.9×10^{19} N m with M_W=6.8. From the distribution of final static displacement and slip angle of each sub-fault (Figure 5) and from the rupture snapshots of every second (Figure 6), the rupture process can be seen to be relatively simple. Starting from the initial point, it extended rapidly upwards, forming a bilateral side rupture feature. The area that released most of the moment was concentrated within a region of 40 km× 30 km, with the largest slip reaching 1.8 m. There was no displacement around the epicenter on the surface. This was consistent with the post-earthquake field investigation. Ground displacement only appears at places 20 km away from the epicenter on its southwest and northeast side, with slip less than 40 cm and the slip direction being southwest and northeast, respectively.

Figure 7(a) shows the final static slip projected onto the surface. The grey dots represent earthquakes that occurred from April 19, 2012 to April 19, 2013. It is clear that the seismicity was low around the M_S7.0 Lushan source region before the Lushan earthquake took place, but it was high in the Wenchuan source region, where many aftershocks of Wenchuan earthquake clustered. Figure 7(b) shows the aftershocks of the Lushan event that took place before April 30. Most of these aftershocks clustered around the large slip area.

5 Discussion and conclusion

According to the present study, the rupture process of Lushan M_S7.0 earthquake was relatively simple. The scale

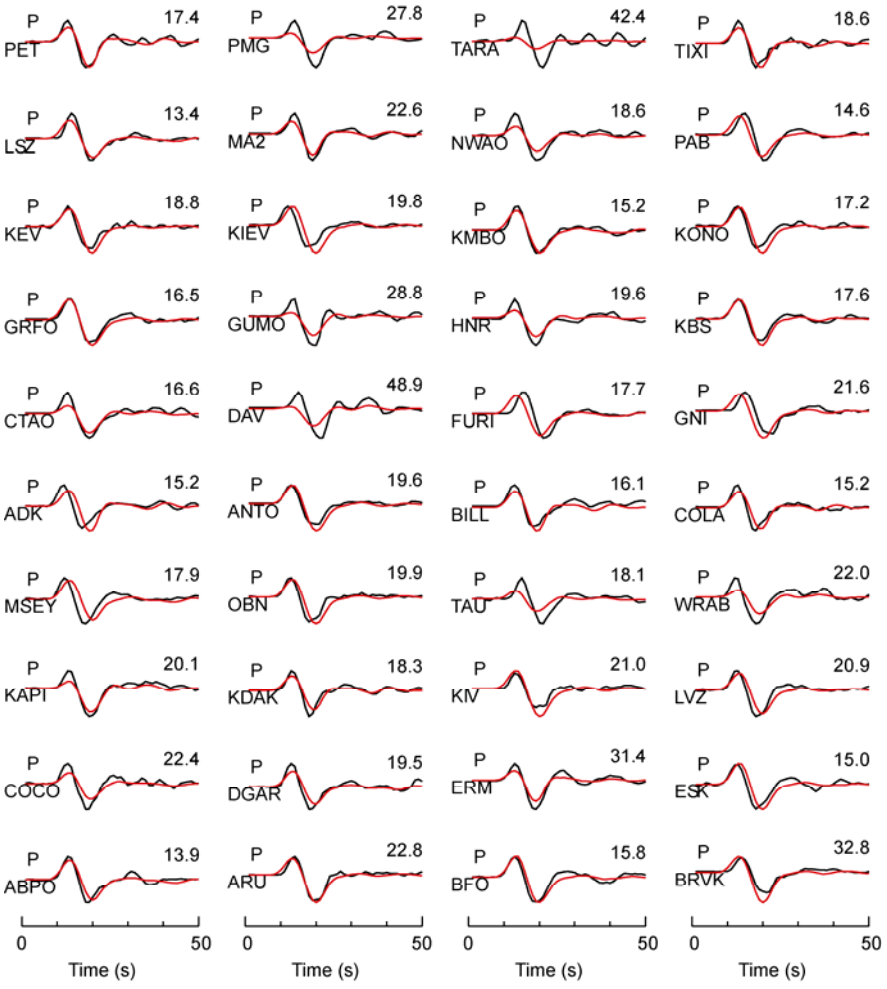

Figure 3 Comparison of the observed waveform data (black) to synthetic data (red).

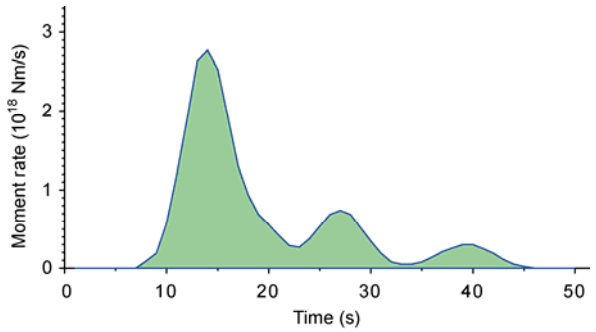

Figure 4 Source time function.

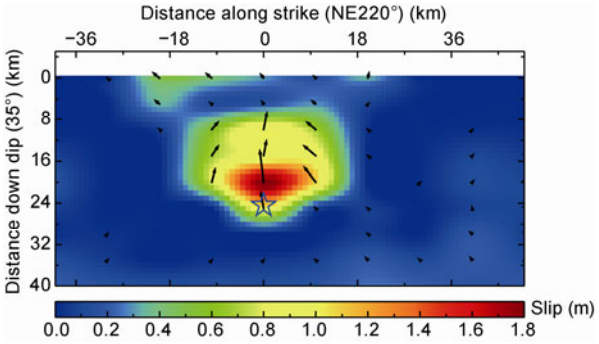

Figure 5 Final static slip distribution on the fault plane. The star indicates the initial rupture point. Black arrow marks the slip vector and its length proportional to the slip value. The maximum slip was 1.8 m.

of the rupture was relatively small. The seismic moment was released during the first 13 s, with a total amount of 1.9 × 10^{19} N m and a moment magnitude M_W of 6.8. The rupture demonstrated a rapid development from the starting point to the surface, showing bilateral rupture characteristics. The large slips generated by the rupture were mainly concentrated around the 40 km × 30 km region above the initial rupture point and had a maximum slip of 1.8 m. No significant slip was found on the surface near the epicenter of the Lushan earthquake, which located 20 km away to the southwest and northeast of the epicenter and showed a slip of less than 40 cm. The directions of these slips were also southwest and northeast, respectively. These inversion results are consistent with the post-earthquake geological survey (http://www.e-igl.ac.cn/wwwroot/c_000000090002/d_0976.html). The geological investigation confirmed that no surface rupture was present on the surface of source region and inferred that the Lushan earthquake was a typical blind faulting earthquake.

The rupture process of the Lushan earthquake differed significantly from that of Wenchuan earthquake [1,14,15]. The rupture process inversion results of Wenchuan earthquake revealed that along the surface of the main central Longmenshan fault zone, there exists a number of large rupture zones. The rupture process of Wenchuan earthquake was decomposed into a series of several M>7 earthquakes ruptures, which were mainly unilateral ruptures in the NE

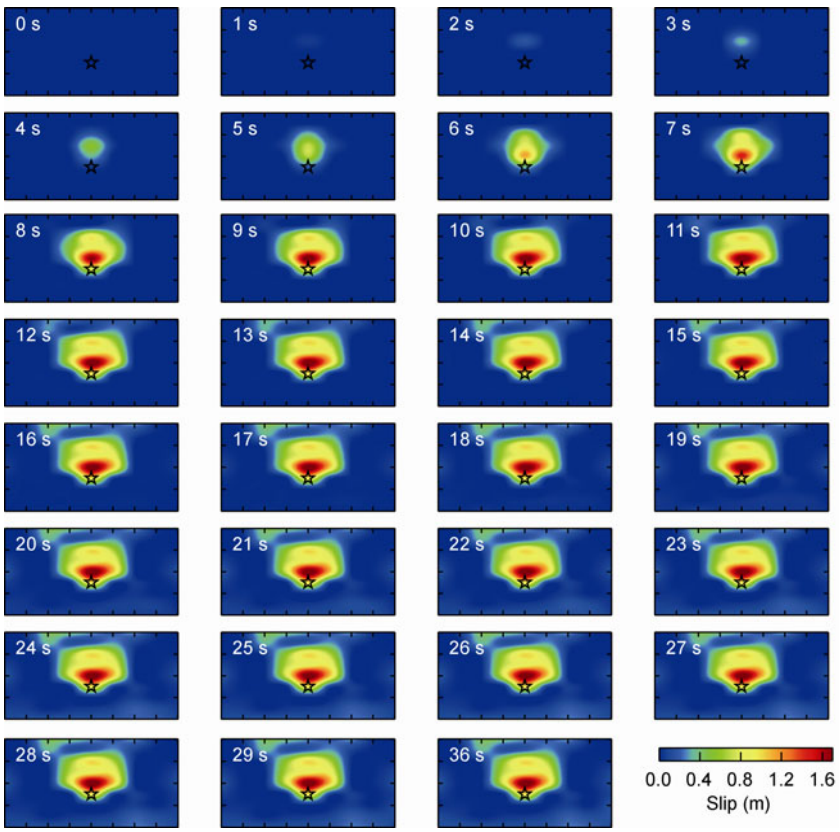

Figure 6 Snapshots of rupture scenario at every second on the fault plane. The star indicates the initial rupture point.

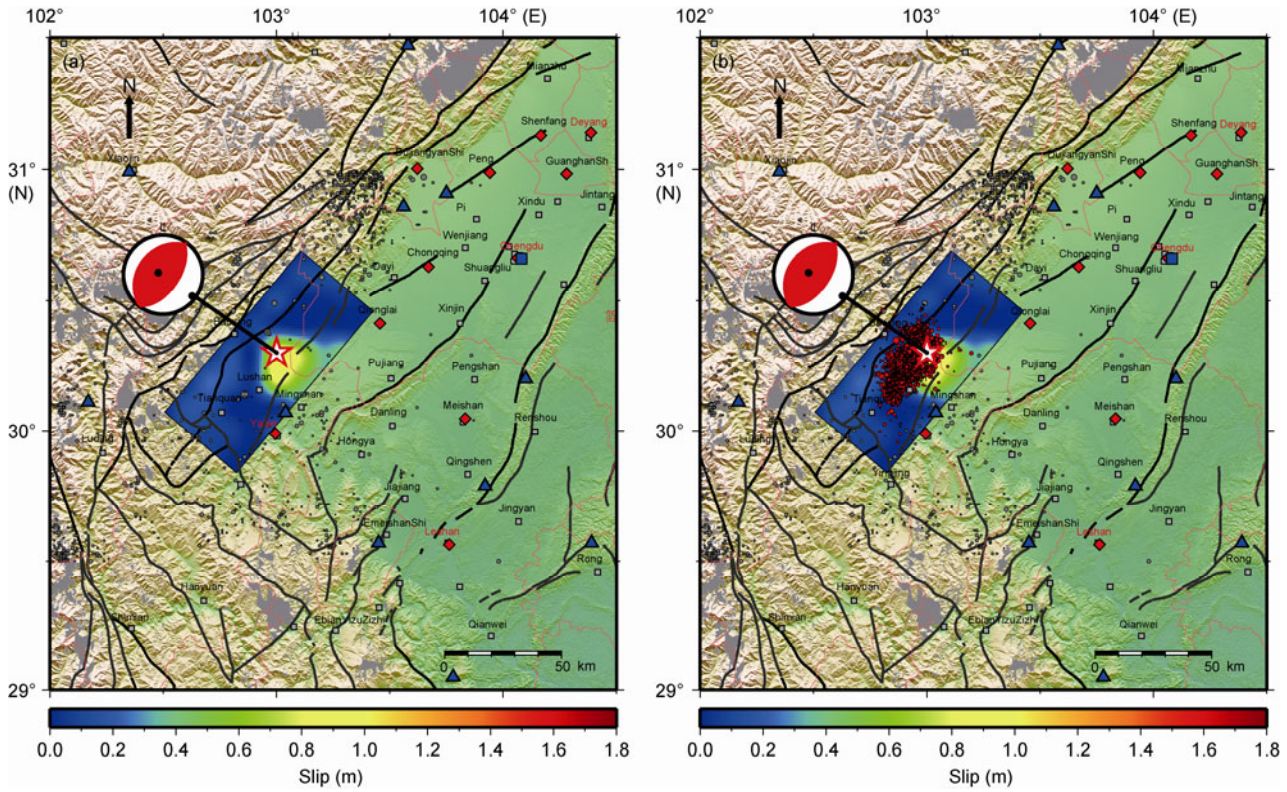

Figure 7 Surface projection of the final slip distribution and finite fault model. Grey dots indicate earthquakes that took place during the year preceding the Lushan M_S7.0 earthquake. Red dots indicate aftershocks that took place before May 4, 2013. The star represents the epicenter.

direction. The overall rupture length reached 330 km. From southwest to northeast, the rupture mode changed from thrust into strike-slip. Geological survey reported that the Wenchuan earthquake, which was a great intra-continental thrust earthquake, produced a number of large surface rupture zones. This great earthquake caused the Beichuan-Yingxiu and Guanxian-Jiangyou faults in the middle section of the Longmenshan fault zone and NW-trending Xiaoyudong fault to rupture simultaneously, so forming two nearly parallel Beichuan-Yingxiu and Hanwang-Bailu surface rupture zones in the NE direction and the Xiaoyudong surface rupture zone in the NW direction. A 240 km long surface rupture zone formed along the Yingxiu-Beichuan fault in the middle section of Longmenshan fault zone, where the observed maximum vertical dislocation and horizontal right-lateral dislocation were approximately 6.5 and 4.9 m respectively. The Guanxian-Jiangyou fault demonstrated mainly thrust ruptures. The maximum vertical displacement was approximately 3.5 m along this 73 km rupture zone. This feature of the rupture indicated that, before the Wenchuan earthquake, the Longmenshan fault zone was in a locked state under both the eastward push from Tibetan Plateau and the barrier effect from Sichuan Basin and had so accumulated a considerable level of stress. The medium in this tectonic faults zone was very uneven.

In addition to the characteristics of small-scale rupture and lack of distinctive displacement distribution on the surface, another notable feature of Lushan earthquake is that the rupture propagation stopped in the NE direction of less than 20 km to the epicenter, the aftershocks of the Lushan

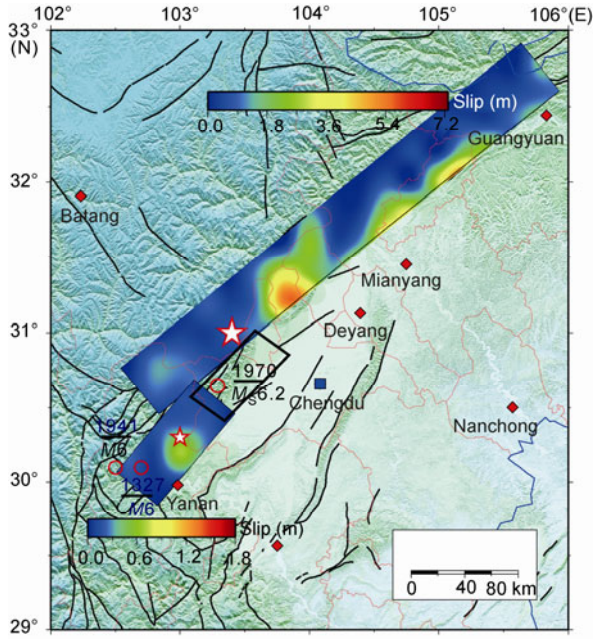

Figure 8 Final static slip distribution on the fault plane both for Wenchuan and Lushan earthquake. Stars represent the epicenters of the Wenchuan and Lushan earthquake, respectively.

earthquake also stopped in the same place (Figure 7(b)). The slip distributions of both the Wenchuan and Lushan earthquakes are projected in Figure 8. As shown, the rupture zones of these two earthquakes were partially connected in the central Longmenshan fault zone. However, on the northeast segment of the Qianshan fault, there was no rupture and aftershocks (the black squares in Figure 8), indicating the significant variance of the medium or the tectonic structure. This may be because of the much stronger medium or some change in structure that prevented the rupture propagation and impeded the aftershock activity.

Although one M_S6.2 earthquake occurred in the middle of this empty segment in 1972, Chen et al. [16] argued that the energy released by this earthquake was less than the amount of energy that could released by an earthquake of the scale equal to the length of the empty segment, that is, an M_W6.8 earthquake. Therefore, further study should be carried regarding the fault structure and medium properties of this segment.

The authors thank the two anonymous reviewers for their helpful comments and suggestions. Seismic data were downloaded from IRIS Data Center, and the figures were drawn using GMT. This work was supported by the National Natural Science Foundation of China (41104033) and the Basic Research Project of Institute of Earthquake Science, CEA (2011IES010104).

1 Zhao C P, Chen Z L, Zhou L Q, et al. Rupture process of the Wenchuan *M*8.0 earthquake of Sichuan, China: The segmentation feature. Chin Sci Bull, 2010, 55: 284–292
2 Xu X W, Chen G H, Yu G H, et al. Reevaluation of surface rupture parameters of the 5.12 Wenchuan earthquake and its tectonic implication for Tibetan uplift (in Chinese). Chin J Geophys, 2010, 53: 2321–2336
3 Zhang P Z, Wen X Z, Xu X W, et al. Tectonic model of the great Wenchuan earthquake of May 12, 2008, Sichuan, China (in Chinese). Chin Sci Bull (Chin Ver), 2009, 54: 944–953
4 Bai D H, Meju M A, Unsworth M J, et al. Crustal deformation of the eastern Tibetan plateau revealed by magnetotelluric imaging. Nat Geosci, 2010, doi: 10.1038/NGEO830
5 Fei Q. Characters of deep structure for Wenchuan earthquake (in Chinese). Chin J Eng Geophys, 2008, 5: 387–395
6 Zhou L Q, Zhao C P, Xiu J G, et al. Tomography of *Q*Lg on Sichuan-Yunnan region (in Chinese). Chin J Geophys, 2008, 51: 1745–1752
7 Wang C Y, Lou H, Lü Z Y, et al. S-wave crustal and upper mantle's velocity structure in the eastern Tibetan Plateau-Deep environment of lower crustal flow. Sci China Ser D-Earth Sci, 2008, 51: 263–274
8 Xu X W, Wen X Z, Ye J Q, et al. The M_S8 Wenchuan earthquake surface ruptures and its seismogenic structure (in Chinese). Seismol Geol, 2008, 30: 597–629
9 Jin W Z, Tang L J, Yang K M, et al. Deformation and zonation of the Longmenshan fold and thrust zone in the western Sichuan basin (in Chinese). Actc Geol Sin, 2007, 81: 1072–1080
10 Kikuchi M, Kanamori H. Inversion of complex body waves-III. Bull Seism Soc Am, 1991, 81: 2335–2350
11 Kikuchi M, Kanamori H, Satake K. Source complexity of the 1988 Armenian earthquake: Evidence for a slow after-slip event. J Geophys Res, 1993, 98: 15797–15808
12 Zhao C P, Chen Z L, Zheng S H, et al. Study on the rupture process of the Sep 27, 2003 M_S7.9 earthquake on the border area of China, Russia and Mongolia. Acta Seismol Sin, 2005, 18: 255–268
13 Zhao C P, Chen Z L, Zhen S H. Source rupture process of 3 Jiashi M_S6 events (1998–2003) and its correlation with aftershock activity. Chin J Geophys, 2008, 51: 774–783
14 Wang W M, Zhao L F, Li J, et a1. Rupture process of the 8.0 Wenchuan earthquake of Sichuan, China (in Chinese). Chin J Geophys, 2008, 51: 1403–1410
15 Zhang Y, Feng W P, Xu L S, et al. Temporal and spatial rupture process of 2008 Wenchuan great earthquake. Sci China Ser D-Earth Sci, 2009, 52: 145–154
16 Chen Y T, Yang Z X, Zhang Y, et al. From 2008 Wenchuan earthquake to 2013 Lushan earthquake (in Chinese). Sci Sin Terrae, 2013, 43:1064–1072